Open Ceramics 21 (2025) 100728

Contents lists available at ScienceDirect

Open Ceramics

journal homepage: www.sciencedirect.com/journal/open-ceramics

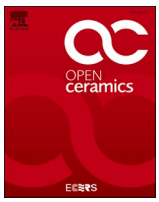

Influence of the binder composition on the water debinding properties of a PVB-PEG-alumina feedstock for the fused deposition of ceramic process

Thomas Heim [a,*], Frank Kern [a,*], Cristina Siligardi [b]

[a] Institute for Manufacturing Technologies of Ceramic Components and Composites (IFKB), University of Stuttgart, Allmandring 7B, 70569 Stuttgart, Germany
[b] Department of Engineering "Enzo Ferrari", University of Modena and Reggio Emilia, Via Pietro Vivarelli 10, Modena 41125, Italy

ARTICLE INFO

Keywords:
Ceramic additive manufacturing
Solvent debinding
Highly filled alumina feedstock

ABSTRACT

The study investigates the influence of several binder compositions on the solvent debinding characteristics of highly filled thermoplastic alumina feedstocks at different temperatures. All feedstocks contain the same powder volume fraction but vary in the repartition of the binder components: polyvinyl butyral (PVB), polyethylene glycol (PEG), and a plasticizer (3G8). The weight loss, debinding speed, volumetric changes, and the microstructure were analyzed. The water temperature was set to room temperature –RT– (23°C) and 40°C. SEM micrographs were taken on as-processed and solvent-debinded samples fractured after dipping in liquid nitrogen. Water debinding of the compositions with high proportions of low molecular weight components PEG and 3G8 helps to reduce the remaining polymer amount and to achieve an open porosity, which should ease the following thermal debinding.

1. Introduction

The material extrusion (MEX-TRB/C/Al_2O_3) [1], or more precisely the material extrusion additive manufacturing of ceramic — further called in this work the Fused Deposition of Ceramics (FDC) process — uses thermoplastic polymers only as auxiliary materials, in contrast to Fused Deposition Modeling (FDM). The thermoplastic polymers in FDC are often summarized as binder or binder systems. The latter implies that the binder is not a single polymer but a mixture of different components. The tasks of the binder are to facilitate thermoplastic shaping and to retain the integrity of the shaped component. Before sintering of the component, the binder has to be removed. Hence the proper selection of binder polymers and the compounding process, aiming at a homogeneous distribution of ceramic particles in the binder are crucial for the success of the manufacturing process. The requirements for binders cannot be met with typical polymers used in FDM. In detail the requirements for the binder for highly filled ceramic filaments include: compatibility and wetting with ceramic powder, limited solubility of the components in each other for two-or more component binders, appropriate thermal stability and thermal decomposition properties [2], low viscosity, low thermal expansion coefficient, good adhesion between deposited layers, elasticity in the green state and high yield strength [3,4]. Non-toxicity of the binder itself during processing and its decomposition products during debinding helps to fulfill workplace security and environmental requirements and increases the acceptance of FDC in industrial applications.

The binder composition may have counteracting effects with respect to the process chain. For example, low-molecular-weight binders produce less gas during decomposition, simplifying the debinding, but are often less viscous than high-molecular-weight binders and reduce the green strength [5,6] and thus the filament strength. Furthermore, since the parts should be chemically surface treated, all binder components need to be soluble in the same solvents.

As in most ceramic manufacturing processes that use higher amount of polymers for the shaping (injection molding, some additive manufacturing processes, etc.), not only the shaping step itself, but also the subsequent debinding process is critical [7]. Defects occurring during the debinding step negatively impact the geometric accuracy; they remain after the sintering step and compromise the mechanical properties of the final part [8]. The components of the binder should be removed successively to reduce the occurrence of defects [7]. A prerequisite for a fast and trouble-free debinding is the so-called two-stage debinding. A part of the binder is dissolved in a solvent, while the remaining part, the so-called "backbone" holds the partially debinded ceramic in shape. This "backbone" is subsequently removed during the second thermal and in most cases oxidizing debinding stage. The ratio

* Corresponding authors.
E-mail addresses: thomas.heim@ifkb.uni-stuttgart.de (T. Heim), frank.kern@ifkb.uni-stuttgart.de (F. Kern).

https://doi.org/10.1016/j.oceram.2024.100728
Received 14 October 2024; Received in revised form 22 November 2024; Accepted 10 December 2024
Available online 11 December 2024

between soluble polymer and insoluble backbone polymer in the binder has an influence on defects [9,10]. During the binder extraction with solvents, a fraction of the solvent may be incorporated into the polymers creating inhomogeneous volumetric variations leading to internal stresses. These stresses may cause cracking or could cause delamination [11,12].

In this study compositional variations in a three-component model binder system, consisting of PVB (polyvinyl butyral), PEG (polyethylene glycol), and a plasticizer, are investigated systematically. This polymer combination is described in the literature for the "non-solvent induced phase separation process" (NIPS) or for use as injection molding feedstock for ceramic and metallic powders [9,13–19]. There is limited literature on the preparation of this binder system for FFF (Fused Filament Fabrication) [20] or FDC [21]. As in a previous work [22], the agitation granulation technique is used as a quick and homogeneous premixing procedure for the feedstock constituents.

PVB is a polar terpolymer of vinyl butyral, vinyl alcohol and vinyl acetate. With or without plasticizer, it is commonly used as backbone constituent in binder systems for several ceramic processing techniques. The properties of PVB i.e. water resistance, thermal degradation behavior, compatibility with non-polar polymer, and interaction with the oxide ceramics depend on the content of chemical functionalities (hydroxyl and acetate) and the molecular weight of the polymer [16–25.

PEG is widely used as a soluble component for the solvent debinding step in highly filled ceramic feedstocks [26]. Two processes drive this debinding step: dissolution and diffusion. In the dissolution step, due to bonding between water and the polymer chains, the PEG forms hydrated complexes and dissolves. Thereby pores are created for the second (diffusion) step. In the diffusion step the PEG diffuses through the solvent-filled pores to the surface of the sample [11,12–27]. Depending on the distance of the dissolving front to the surface, the dissolution or diffusion are successively the rate-limiting steps [12]. Solvent temperature plays a crucial role in the debinding speed. At higher temperatures – above 30°C– solubility increases but defects such as swelling may occur [9–11].

As ceramic material, a submicron-size alumina (α-Al_2O_3) powder is used. Alumina is the most important technical oxide ceramic, has the widest range of applications, and is well documented. Dense-sintered alumina exhibits high strength and hardness, good temperature stability, high wear and corrosion resistance even at elevated temperatures [28]. The high-purity alumina used in this work has been successfully utilized for FDC in a previous work [22] and sinters to a high density at 1550-1600°C [29,30].

The influence of the aforementioned binder composition on debinding speed, defects and volumetric changes during the solvent debinding will be investigated in this work.

2. Materials and methods

2.1. Materials

The ceramic powder used in this study is a high-purity alumina (CT 3000 LS SG, Almatis GmbH, Frankfurt, Germany). According to the manufacturer, the powder has a particle size of 0.5 μm D_{50} and 2 μm D_{90} and a surface area of 7.8 m^2/g. As a sintering additive, 1500 ppm spinel powder S30 CR (Baikowski, Poisy, France) was added, this corresponds to 500 ppm MgO.

For the binder the Mowital® PVB resin grade 75H (Kuraray Europe GmbH, Hattersheim, Germany) in the form of fine powder and PEG 6000 (Tecnaro GmbH, Ilsfeld, Germany) were used. As plasticizer for the PVB resin, triethylenglycol-di-(2-ethylhexanoate) with commercial name OXSOFT 3G8 Cereplas DOA, provided by Krahn Ceramics (Krahn Ceramics GmbH, Hamburg, Germany), was used.

2.2. Feedstock preparation

The compositions of the feedstocks were defined volumetrically by the simplex centroid mixture design (cf. Fig. 1 and Table 1). The theoretical density of PVB, PEG, 3G8, and alumina powders for the calculation were respectively set to 1.2 g/cm^3, 1.2 g/cm^3, 0.967 g/cm^3, and 3.94 g/cm^3.

Feedstock 1 was produced twice (called feedstock 1 and 1.2), in order to verify the reproducibility of the compounding process.

The feedstocks were manufactured according to the process developed in a previous work (process V1 [22]) but with different polymers. All the constituents were added together into the recipient: PVB in the form of fine powder and the ceramic powders with the PEG flakes and the liquid 3G8 with 80 ml distilled water. The mixing was done in an Eirich R02 mixer (Maschinenfabrik Gustav Eirich, Hardheim, Germany). After an initial mixing, water was added gradually in 10 ml steps until granulation occurred. The granulated feedstock was then dried for at least 24 hours at 40°C. The feedstock was then homogenized two times through a twin-screw extruder (HAAKE Polylab OS Rheomex PTW16/25 OS, Thermo Fisher Scientific, Karlsruhe, Germany) with temperatures of the segments ranging from 80°C to 160°C. The extrusion nozzle had a rectangular shape with dimensions 2.5 x 4.5 mm.

The homogeneity of the feedstocks was evaluated by collecting five rectangular rods samples, weighing between 1 and 1.8 g, randomly along the extruded strands and debinding them thermally at 800°C to assess the ceramic content.

2.3. Water debinding

For each composition, 8 samples with random lengths between 45 mm and 100 mm were collected at different positions along the extruded line, to ensure better representativeness. For the feedstock 1.2, three series of 8 samples of the same feedstock were taken, resulting in 24 samples in total. The samples were weighed, and the cross section was measured in three marked positions with an Orion electronic caliper (HAHN+KOLB Werkzeuge GmbH, Ludwigsburg, Germany, accuracy ±0.01 mm). These measurements were done in the as-processed state, and after drying at 40°C for 72h to remove the absorbed water. The samples were then debinded in 4 liters of stationary distilled water at RT (23°C) and at 40°C. The samples were fixed in vertical position in the water bath with a support structure to guarantee a uniform contact to solvent on all sides and to maintain the same distance between the

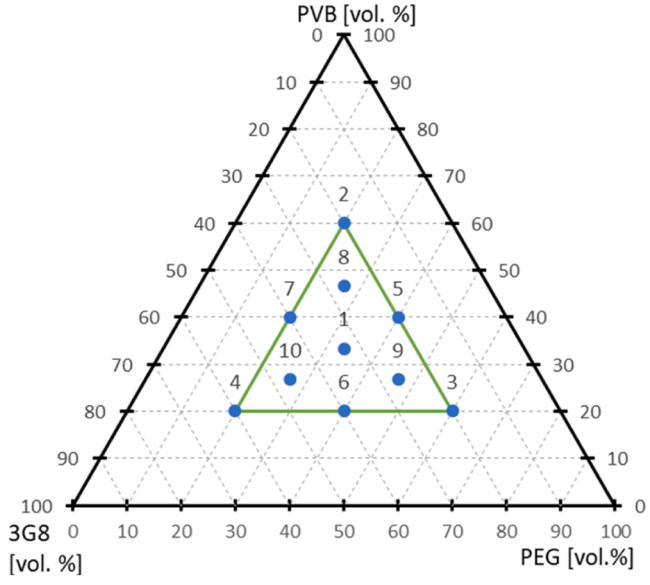

Fig. 1. Ternary plot with the binder composition of the feedstocks 1-10.

Table 1
Binder composition of the binders 1-10.

Feedstock	Binder						Powder	
	PVB	[vol. %]	PEG	[vol. %]	Plasticizer	[vol. %]	Alumina	[vol. %]
1	PVB 75H	16.67	PEG 6000	16.67	3G8	16.67	CT3000LSSG	50
2	PVB 75H	30	PEG 6000	10	3G8	10	CT3000LSSG	50
3	PVB 75H	10	PEG 6000	30	3G8	10	CT3000LSSG	50
4	PVB 75H	10	PEG 6000	10	3G8	30	CT3000LSSG	50
5	PVB 75H	20	PEG 6000	20	3G8	10	CT3000LSSG	50
6	PVB 75H	10	PEG 6000	20	3G8	20	CT3000LSSG	50
7	PVB 75H	20	PEG 6000	10	3G8	20	CT3000LSSG	50
8	PVB 75H	23.33	PEG 6000	13.33	3G8	13.33	CT3000LSSG	50
9	PVB 75H	13.33	PEG 6000	23.33	3G8	13.33	CT3000LSSG	50
10	PVB 75H	13.33	PEG 6000	13.33	3G8	23.33	CT3000LSSG	50

samples. Both recipients had a lid to limit the evaporation. The 40°C water bath was placed in the oven until the required temperature was reached. The temperature was verified with an electronic digital thermometer.

Then one sample of each feedstock composition was withdrawn from the water bath after 1, 2, 3, 4, 5, 8, 25, and 50 hours. Directly after the withdrawal from the debinding bath, the samples were measured, placed flat in a recipient and after drying for 72 hours at 40°C weighed again.

2.4. Calculations

The proportion of the binder dissolved and evaluated relative to PEG content were calculated as follows:

$$wt_{b.dis.} = \frac{(wt_{dried1} - wt_{dried2})}{wt_{dried1}}$$

$$wt_{PEG.dis.} = \frac{(wt_{dried1} - wt_{dried2})}{wt_{PEG1}}$$

Here, $wt_{b.dis.}$ is the relative weight loss after water debinding in [wt. %], wt_{dried1} and wt_{dried2} are the weight of the sample in [g] after drying at 40°C for 72 hours respectively before and after the water debinding step. $wt_{PEG.dis.}$ is the relative weight loss after water debinding compared to the initial PEG content in [wt.%], and wt_{PEG1} is the weight of PEG in the initial composition in [g].

The debinding speed was calculated as the mean of the relative weight loss divided by the time between each sample withdrawal. The calculation is only applied to the first eight hours of debinding.

The swelling and shrinkage of the samples were calculated were calculated as follows:

$$dim_{rel.1} = \frac{(dim_{dried1} - dim_{deb.})}{dim_{dried1}}$$

$$dim_{rel.2} = \frac{(dim_{dried1} - dim_{dried2})}{dim_{dried1}}$$

Here, $dim_{rel.1}$ is the relative dimension change in the soaked condition in width and height in [%]. dim_{dried1} and dim_{dried2} are the dimensions of the samples after drying at 40°C for 72 hours respectively before and after the water debinding step in [mm]. $dim_{deb.}$ is the dimension of the samples right after exiting the debinding bath; $dim_{rel.2}$ is the relative dimension change after the solvent debinding step in [%].

2.5. Ternary diagrams

The ternary diagrams in the results section were created using the OriginLab 2016 (OriginLab Corporation, Northampton, USA) software. The values in the planes between the measurement points result from the linearization.

2.6. Microscopy

The SEM micrographs were taken on a JEOL JSM-6490LV (JEOL (Germany) GmbH, Freising, Germany). The fracture surface of the cross section of the middle point and the edges of the test matrix were evaluated (Feedstocks 1, 2, 3, and 4, cf. Fig. 1, and Table 1). To reduce the plastic deformation, which could modify the microstructure, the samples in green state were dipped in liquid nitrogen to achieve a brittle fracture before being broken. Half of the samples were then solvent debinded in water for 48 hours at room temperature(RT). To assess the effect of nitrogen dipping, one Feedstock 1 sample was fractured at room temperature.

3. Results

3.1. Feedstock processing

All the feedstocks were successfully extruded. For the first homogenization step, the rotation speed of the extruder needed to be adapted to prevent reaching the maximum torque of the extruder. After extrusion and from a visual point of view, all the feedstocks are very similar.

The powder is homogeneously distributed among the sample without segregation as displayed on the back-scattered SEM image in the Fig. 2.

The extruded strands have an average width of 3.91 ± 0.15 mm and an average height of 2.28 ± 0.1 mm. Hence, compared to the nozzle diameter, a contraction of ~13% occurred.s

All the feedstocks with more than one-third of plasticizer volume content reacted with the other polymers in contact, like the polystyrene cups or the filament spools (cf. Fig. 3).

Note: Since the feedstocks are designed volumetrically and the binder constituents do not have the same density, the weight content of the powder differs while the volume content is identical. Fig. 4 shows the weight percentage of the ceramic powder measured after thermal debinding in comparison to the theoretical weight percentage. The

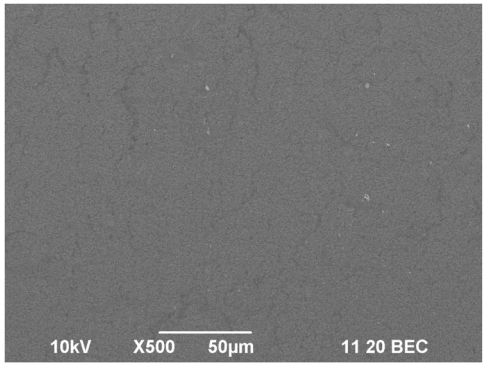

Fig. 2. Back-scattered SEM micrographs of the cross section of Feedstock 1 broken at RT at mag. x500.

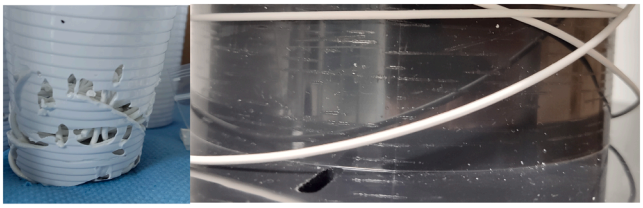

Fig. 3. Plasticizing effect of the 3G8 from the feedstocks with the plastic parts that comes incontact.

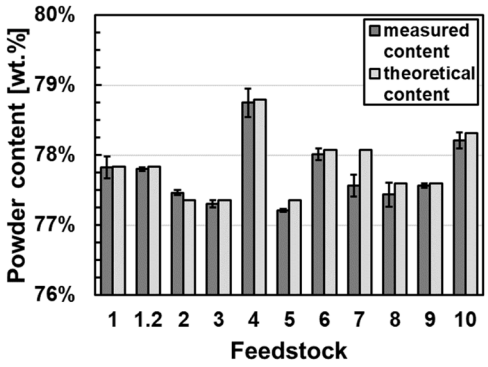

Fig. 4. Actual and theoretical ceramic powder weight content in the feedstocks.

theoretical and measured solid content, as well as the standard deviation, are in good accord, which indicates a good homogeneity of the feedstocks.

3.2. Water debinding

Depending on the binder composition, there are differences both in maximum weight loss and debinding speed. Fig. 5 shows the cumulative average of the relative PEG weight loss for the feedstocks. The initial mass loss after one hour is higher at 40°C, but the difference tends to decrease with longer debinding time.

Fig. 6 displays the mean relative debinding speed per hour for the first 8 hours. The compositional fields correspond to the area depicted in Fig. 1. The samples with lower PEG and 3G8 content tend to debind slower and reach lower weight losses after 50 hours of debinding time (Fig. 7). For both debinding temperatures, the samples with the highest PVB (Feedstock 2) have the minimum debinding speed of 1.4 PEG%/h at RT and 1.5 PEG%/h at 40°C. The maximum debinding speed is reached by the samples with the most PEG content (Feedstock 3) with respectively 14.4 PEG%/h at RT and 13.1 PEG%/h at 40°C. For the four series of the feedstock 1, which lies in the center point of the test matrix, the

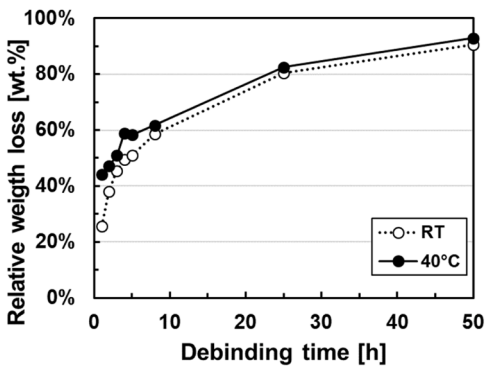

Fig. 5. Mean weight loss relatively to the initial PEG content of the feedstocks 1-10 during water debinding at RT and 40°C.

mean of the aforementioned debinding speed is 8.9 ± 0.7 PEG%/h for debinding at RT and 11.3 ± 0.3 PEG%/h for debinding at 40°C.

Fig. 7 shows the relative mass loss after 50 hours debinding time for each feedstock at room temperature and at 40°C. This comparative value can be considered as an equilibrium state in which all the accessible soluble parts are extracted. Some values exceeding the weight percentage of PEG, especially the samples with higher plasticizer content (Feedstocks 4 and 10), suggest that other components of the feedstock have been leached out together with the PEG. As foreseeable, the samples with the highest PEG contents show higher absolute weight losses. The samples of feedstock 3 have a total weight loss of 13.24 wt.% at RT and of 14.01 wt.% at 40°C, which is close to the total amount of PEG contained in the feedstock (14.14 wt.%). For the Feedstock 2, with the lowest amount of PEG and plasticizer, the weight loss after 50 hours debinding time is only 2.01 wt.% at RT and 2.77 wt.% at 40°C, which is much lower than the 4.71 wt.% of PEG contained in the material. The mean values for the Feedstock 1 (central point) are 7.1 ± 0.3 wt.% at RT and 6.9 ± 0.3 wt.% at 40°C.

Fig. 8 presents the maximum swelling or shrinkage of the samples. For most of the feedstocks, this maximum dimensional change is attained after 5 hours for the debinding at 40°C and after 50 hours for the debinding at RT. The feedstocks 2, 7, and 8 (containing the lowest PEG fraction) present a shrinkage behavior. For the samples from the Feedstock 1 (central point) the mean values of the size variation are 2.08 ± 0.3 % for debinding at RT and 2.56 ± 0.2 % for debinding at 40°C. Feedstocks 3 and 9 with the highest PEG contents (lower right corner) exhibit swelling behavior.

On some samples with higher 3G8 contents debinded at 40°C (feedstocks 4 and 10, lower left corner of the triangle) blisters appeared on the surface (cf. Fig. 9). Only one sample presented cracks (feedstock 10) after 50 hours in the water bath at 40°C.

Fig. 10 presents the SEM micrograph of the fracture surface of the Feedstock 1 broken at RT and after dipping in liquid nitrogen. The cross section of the feedstock 1 fractured in liquid nitrogen shows some polymer accumulation over larger areas on the surface. It also seems to present fewer dimples.

The water debinded fracture surfaces of the feedstock 1, 2, 3, and 4 are displayed in Fig. 11. The Feedstock 2 presents the most regular surface with the highest visible polymer amount. On the surface of the feedstocks 3 and 4, one can clearly distinguish individual alumina grains and some open porosity. This open porosity has a size smaller than the grain size of the powder. The Feedstock 1 lies in-between in terms of visible polymer and porosity.

4. Discussion

The feedstocks processing and extrusion were successful even if the feedstocks with more than 33.33 vol.% plasticizer in the binder reacted with the polystyrene containers. This indicates that the plasticizer to backbone-polymer ratio is too high. The low standard deviation of the powder content among the extrudates (Fig. 4) implies that the premixing and the homogenization with the twin screw extruder is sufficient for a homogenous distribution of the ceramic powder in the feedstock. This is further demonstrated by the backscattered SEM micrograph and is a prerequisite for the reliability of further investigations.

The debinding bath was static, but the solvent volume to parts volume should be high enough to neglect the influence of PEG in the solution on the debinding rate [27]. Furthermore, the samples were held vertically in the solvent bath, so the molecules could diffuse easily from the surface of the parts into the surrounding water.

The limitations of this study regarding debinding are twofold. First, due to the high number of feedstocks and parameters, it was not possible to evaluate multiple samples per feedstock in order to effectively differentiate the measurement process variations with the material variations. However, the low standard deviations of the four feedstock 1

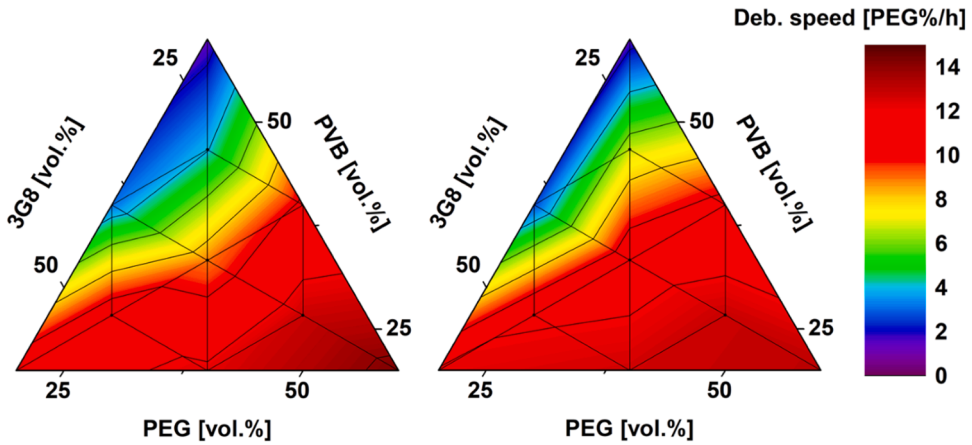

Fig. 6. Mean weight loss of the feedstocks 1-10 relatively to their initial PEG content during the first 8 hours of water debinding at RT (left) and 40°C (right).

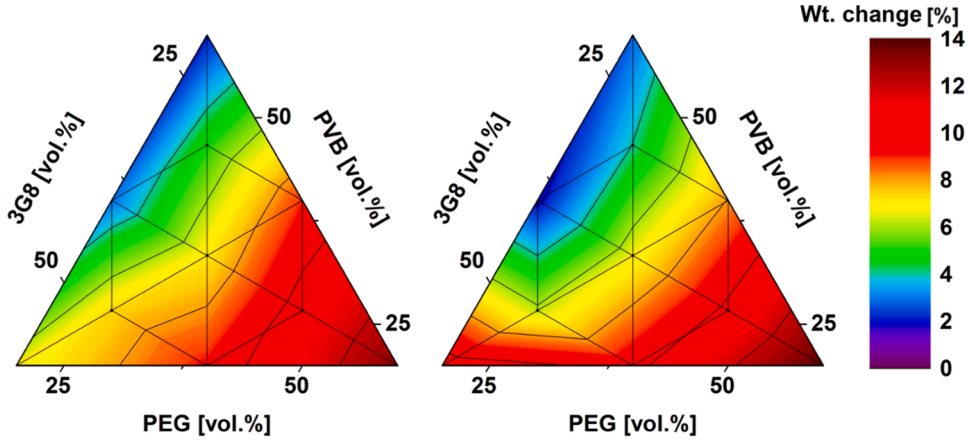

Fig. 7. Relative weight loss of feedstocks 1-10 after water debinding for 50 hours at RT (left) and 40°C (right).

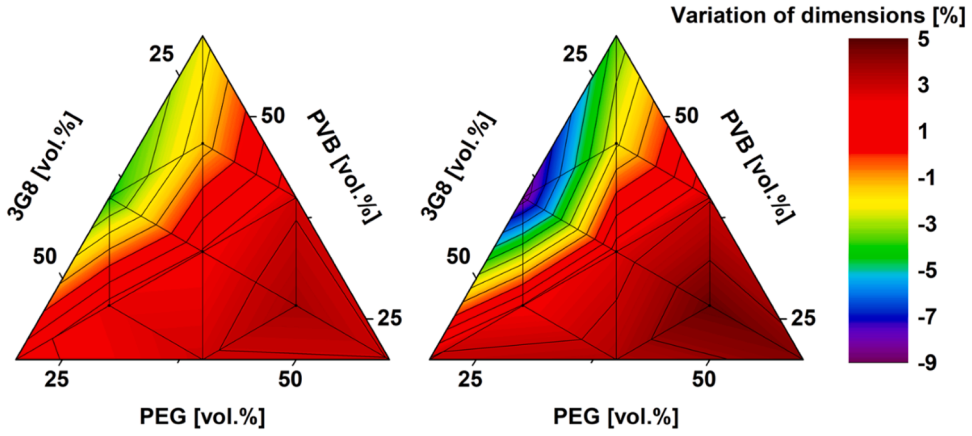

Fig. 8. Relative maximum dimension changes of the feedstocks 1-10 during water debinding at RT (left) and 40°C (right) measured immediately after remoal from the debinding bath.

series for the weight and size changes during debinding confirm the reproducibility of these measurements. Secondly, since some feedstocks being softer than others, especially when soaked with water during the debinding process, the dimension assessments with the caliper limit the precision of the measurements. The precision is also affected by the surface quality of the samples and the strength applied by the caliper. Here a non-tactile measurement or an in-situ measurement as performed by Yang et al. [31] may lead to improvements in accuracy.

There are small changes in the dimensions of the extruded samples. These variations do not influence the debinding values much, since the surface to volume ratio is similar. Thus, the role of the differences in effective length scale between the samples, as shown by Shivashankar and German, can be neglected [12]. The high debinding speed in the first hours, caused by the low diffusion distance of the dissolved polymer to the surface, complies with models stated in the literature [12]. The debinding speed (as shown in Fig. 5) is correlated to the relative PEG

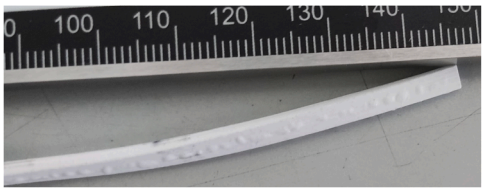

Fig. 9. Blisters on the surface of the feedstock 4 sample after 3 hours water debinding at 40°C.

content. Even if there is more PEG to leach out in the Feedstock 3 compared to the Feedstock 2, the Feedstock 2 is slower to debind. This can be explained by the fact that the diffusion process is affected by the microstructure [32] and the percolation of the pores which limits the access of water towards the center of the part and the diffusion of PEG.

Besides the feedstock composition, the solvent temperature plays an important role in defect-free debinding. Increasing the water temperature of the debinding bath from room temperature to 40°C is beneficial on the one hand, as it tends to increase both debinding speed (Fig. 5) and the maximum relative weight loss (Fig. 7). This is especially relevant for samples with higher plasticizer content, and to a limited extent for the others. This effect relies on the increased dissolution rates and diffusivity of the molecular chains at higher temperatures [11,27]. However, these positive effects can be counterbalanced by higher swelling values (Fig. 8), which could in some applications deform or damage the parts [9] and cause distortion, blisters, cracks, or delamination [9,11]. The higher the temperature, the higher is the thermal expansion [31]. This could also lead to higher stresses in the initial stage of the solvent debinding step or after removing the parts from the debinding bath.

Unexpectedly, the samples with higher plasticizer content tend to have higher total relative weight losses. Even in some cases higher than the PEG content. Since the powder content after solvent debinding is close to the theoretical powder content (cf. Fig. 4), there is no powder loss during solvent debinding. Hence, we assume that plasticizer molecules embedded in the binder have also diffused into the water bath. This effect is magnified by the debinding temperature.

The samples with the highest PEG content tend to have high dimension variations during the water debinding step (cf. Fig. 8). The swelling of the samples depends on the crystal structure of PEG which in turn depends on its molecular weight. PEG 6000, which is used in this study, should have folded chain crystals [10]. However, the still relatively low molecular weight of the PEG allows a fast diffusion of the hydrated polymer complexes to the surface of the sample before defects appear. This interpretation is supported by the fact that structural failure during debinding - such as crack formation - only occurred in the sample with lower backbone to soluble polymer ratio and at higher temperature after prolonged debinding. The blistering mechanism is well described by Yang et. al as the result of internal cracks close to the surface that absorb water [10]. This explanation is consistent with the observation on the extruded samples. After perforation, these blisters release water until they flatten. However only one sample of the studied binder system presented cracks (Feedstock 10) in contrast to their PEG 6000-PMMA binder [9]. However in their study the PEG content of the binder is very high with 65% [10]. The fact that samples containing lower PVB fractions tend to have more defects after remaining for a longer period of time in the debinding bath can easily be explained as less backbone amount means less PVB ligaments, which procure the green strength to the part [9]. To improve the defect resistance of the parts during debinding, even with lower PVB contents, changing the PVB type for higher elongation at break could be a solution. The water intake in PVB has an influence on its mechanical properties. Since the water intake depends on the chemical functionalities of PVB, having a PVB with lower water absorption could enhance the integrity of samples after debinding [33]. Another possibility for reducing the defects could be to debind with a water temperature exceeding the melting temperature of the PEG. However, this could lead to a controversial effect, because of the thermal expansion [31,32]. The negative volumetric changes (shrinkage) in the samples with lower PEG (cf. Fig. 8) could be explained by the release of internal stresses (e.g. by curling of stretched polymer chains) after dissolution of the PEG. This effect should be further investigated.

Breaking the feedstock in liquid nitrogen resulted in changes of the surface of the samples. The polymer that accumulated on the sample surface must be PEG since it disappears after solvent debinding (cf.

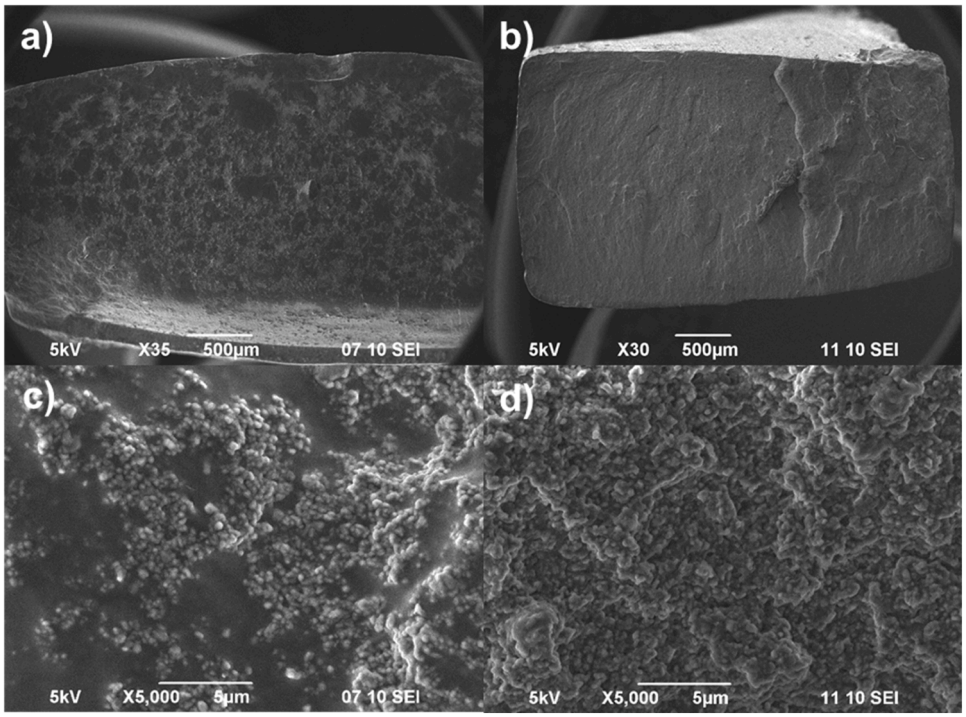

Fig. 10. SEM micrographs of the cross sections of the Feedstock 1 fractured after dipping in liquid nitrogen (a) and (c), and fractured at RT (b) and (d).

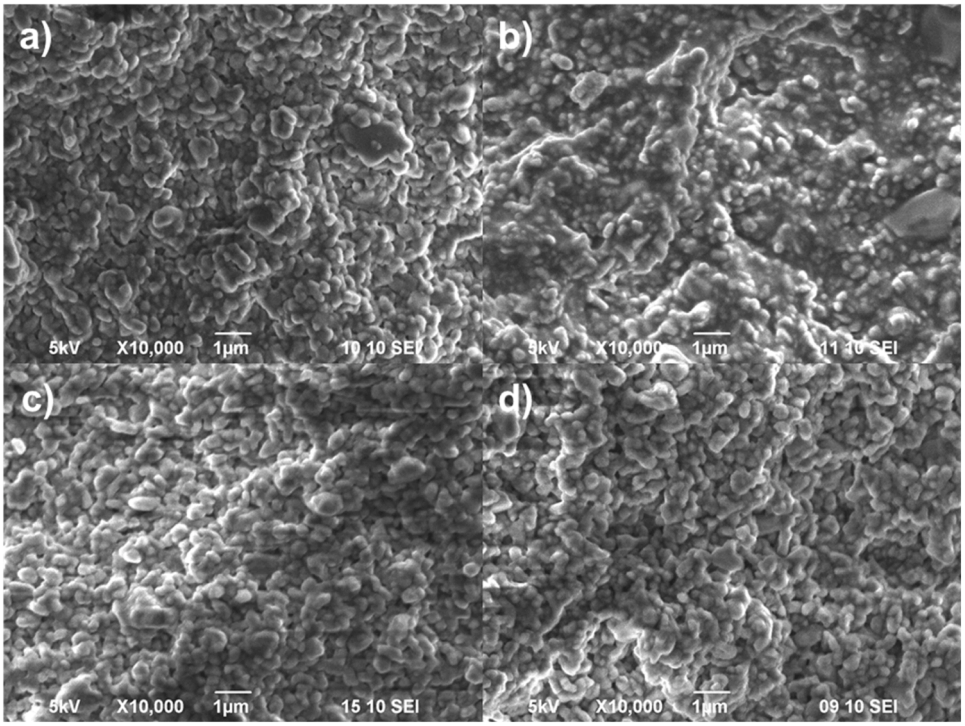

Fig. 11. SEM micrographs of the cross sections of the feedstocks 1-4 after water debindingat RT for 48 hours – Feedstock 1 (a), Feedstock 2 (b), Feedstock 3 (c), and Feedstock 4 (d).

Fig. 10, and Fig. 11). After dipping in liquid nitrogen, the cold samples probably led to condensation. While the samples reaches again the room temperature, this water deposited on the surface, from the previously mentioned condensation, can diffuse inside the sample. This water intake increase the mobility of the PEG molecules and in turn led to its the diffusion toward the surface. The use of liquid nitrogen helps to have a fracture surface which is representative to the inner structure of the sample. However, after dipping the samples, they should be kept in vacuum or in a desiccator to avoid water intake and the diffusion of PEG to the surface.

There is a strong inverse correlation between the PVB amount and the open porosity visible in Fig. 11. This correlates with the measured values in Fig. 7. The fact that there is no powder loss during water debinding, and that the porosity remains between the grains denote that the microstructure of the PVB-PEG-3G8 blend is relatively small compared to the grain size. High amount of the plasticizer 3G8 also lead to a high open porosity, as can be seen from the cross-section micrographs (cf. Fig. 11). However, the drawback is that it reacts with the surrounding polymeric materials, making it more difficult to process.

5. Conclusion

Feedstocks for the Fused Deposition of Ceramic of alumina with a new PVB-PEG-plasticizer composition were successfully processed and partially debinded in water. There is a homogeneous distribution of the 50 vol. % powder among the feedstock.

Time, temperature and initial PEG and plasticizer contents influence the debinding process.

A binder with a major part of both PEG or 3G8 (plasticizer) will have a higher debinding speed and an increased weight loss during debinding, but will also have high swelling during debinding. Feedstocks with low PEG content may have volume reduction during solvent debinding.

Increasing the water bath temperature, increases the debinding speed, the volume changes, and the maximum debinded amount. The latter effect is especially visible on feedstocks with higher plasticizer contents. This binder composition does not promote solvent debinding defects. Only the lack of mechanical stability from lower PVB content can cause defects after debinding for a longer time at 40°C.

Breaking the green samples in nitrogen produces a fracture surface with less plastic deformation, but leads to the diffusion of the water-soluble components to the surface of the sample, which changes the polymer repartition and hinders the correct interpretation. This technique would only be beneficial for studying the microstructure after solvent debinding or on binders which do not react with water.

The microstructure of the solvent debinded green feedstocks are in accordance with the gravimetric study: reducing the PVB amount in the binder increases the amount of polymer removed, increases the amount of open porosities, which should ease the thermal debinding step. However, a certain amount of PVB is still necessary to bring strength to the feedstock and to avoid defects during solvent debinding.

Since thermal debinding is the bottleneck of the process, even longer solvent debinding times of more than 50 hours can be considered as relatively short. The focus should be set on maximum weight loss and defect free debinding.

This binder composition can be an eco-friendlier substitute of the conventional acetone-debinded feedstocks.

Debinding characteristics represent only one of key properties for successful fabrication of the parts. Further study will be done on the influence of the composition on the green mechanical properties and the rheology of the feedstocks.

Funding

The authors would like to thank the Ministry of Science, Research and Arts of the Federal State of Baden-Württemberg for the financial support of the projects within the Innovations Campus Future Mobility (ICM)

The authors are grateful to the JECS Trust for funding the visit of Thomas Heim to DIEF UNIMORE Contract No. 2022327

CRediT authorship contribution statement

Thomas Heim: Writing – review & editing, Writing – original draft, Visualization, Validation, Supervision, Software, Resources, Project administration, Methodology, Investigation, Funding acquisition, Formal analysis, Data curation, Conceptualization. **Frank Kern:** Writing – review & editing, Supervision. **Cristina Siligardi:** Writing – review & editing, Supervision.

Declaration of competing interest

The authors declare that they have no known competing financial interests or personal relationships that could have appeared to influence the work reported in this paper.

Acknowledgements

Holger Rühl is thanked for his assistance with the liquid nitrogen dipping process of the samples.

References

[1] DIN EN ISO/ASTM 52900:2022-03, Additive Fertigung_- Grundlagen_- Terminologie (ISO/ASTM 52900:2021); Deutsche Fassung EN_ISO/ASTM 52900: 2021, (n.d.). https://doi.org/10.31030/3290011.
[2] T.F. McNulty, F. Mohammadi, A. Bandyopadhyay, D.J. Shanefield, S.C. Danforth, A. Safari, Development of a binder formulation for fused deposition of ceramics, Rapid Prototyp. J. 4 (1998) 144–150, https://doi.org/10.1108/13552549810239012.
[3] S. Onagoruwa, S. Bose, A. Bandyopadhyay, Fused deposition of deramics (FDC) and domposites, in: 2001. https://doi.org/10.26153/tsw/3267.
[4] M. Allahverdi, S.C. Danforth, M. Jafari, A. Safari, Processing of advanced electroceramic components by fused deposition technique, J. Eur. Ceram. Soc. 21 (2001) 1485–1490, https://doi.org/10.1016/S0955-2219(01)00047-4.
[5] Kuraray mowital, Mowital® – Polyvinyl butyral (PVB) introduction and overview, (2020).
[6] W.-W. Yang, K.-Y. Yang, M.-H. Hon, Effects of PEG molecular weights on rheological behavior of alumina injection molding feedstocks, Mater. Chem. Phys. 78 (2003) 416–424, https://doi.org/10.1016/S0254-0584(02)00203-1.
[7] K. Sharmin, I. Schoegl, Two-step debinding and co-extrusion of ceramic-filled PEBA and EVA blends, Ceram. Int. 40 (2014) 14871–14879, https://doi.org/10.1016/j.ceramint.2014.06.082.
[8] F. Sommer, H. Walcher, F. Kern, M. Maetzig, R. Gadow, Influence of feedstock preparation on ceramic injection molding and microstructural features of zirconia toughened alumina, J. Eur. Ceram. Soc 34 (2014) 745–751, https://doi.org/10.1016/j.jeurceramsoc.2013.09.020.
[9] G. Thavanayagam, J.E. Swan, Aqueous debinding of polyvinyl butyral based binder system for titanium metal injection moulding, Powder. Technol. 326 (2018) 402–410, https://doi.org/10.1016/j.powtec.2017.11.069.
[10] X. Yang, C. Jia, Z. Xie, W. Liu, Q. Liu, Water-soluble binder system based on poly-methyl methacrylate and poly-ethylene glycol for Injection molding of large-sized ceramic parts, Int. J. Appl. Ceram. Technol. 10 (2013) 339–347, https://doi.org/10.1111/j.1744-7402.2011.02745.x.
[11] C. Abajo, A. Jiménez-Morales, J.M. Torralba, New processing route for ZrSiO4 by powder injection moulding using an eco-friendly binder system, Bol. Soc. Esp. Cerámica Vidr. 54 (2015) 93–100, https://doi.org/10.1016/j.bsecv.2015.05.003.
[12] T.S. Shivashankar, R.M. German, EFfective length scale for predicting solvent-debinding times of components produced by powder injection molding, J. Am. Ceram. Soc. 82 (1999) 1146–1152, https://doi.org/10.1111/j.1151-2916.1999.tb01888.x.
[13] Y. Luo, F. Yang, C. Li, F. Wang, H. Zhu, Y. Guo, Effect of the molecular weight of polymer and diluent on the performance of hydrophilic poly(vinyl butyral) porous heddle via thermally induced phase separation, Mater. Chem. Phys. 261 (2021) 124227, https://doi.org/10.1016/j.matchemphys.2021.124227.
[14] V.A. Krauss, E.N. Pires, A.N. Klein, M.C. Fredel, Rheological properties of alumina injection feedstocks, Mater. Res. 8 (2005) 187–189, https://doi.org/10.1590/S1516-14392005000200018.
[15] Z.P. Xie, L.L. Wang, X.F. Yang, Z.T. Zhang, Water debinding for zirconia powder injection molding, Key Eng. Mater. 368 (372) (2008) 732–735, https://doi.org/10.4028/www.scientific.net/KEM.368-372.732.
[16] Y. Thomas, B.R. Marple, Partially water-soluble binder formulation for injection molding submicrometer zirconia, Adv. Perform. Mater. 5 (1998) 25–41, https://doi.org/10.1023/A:1008681920391.
[17] X.F. Yang, Z.P. Xie, G.W. Liu, Y. Huang, Dynamics of water debinding in ceramic injection moulding, Adv. Appl. Ceram. 108 (2009) 295–300, https://doi.org/10.1179/174367608X362430.
[18] V.A. Krauss, A.A.M. Oliveira, A.N. Klein, H.A. Al-Qureshi, M.C. Fredel, A model for PEG removal from alumina injection moulded parts by solvent debinding, J. Mater. Process. Technol. 182 (2007) 268–273, https://doi.org/10.1016/j.jmatprotec.2006.08.004.
[19] N. Chuankrerkkul, P. Sooksaen, P. Pakunthod, T. Kosalwit, W. Pinthong, Powder Injection Moulding of Alumina Using PEG/PVB Binder Systems, Key Eng. Mater. 545 (2013) 173–176, https://doi.org/10.4028/www.scientific.net/KEM.545.173.
[20] R. Eickhoff, S. Antusch, D. Nötzel, T. Hanemann, New Partially water-soluble feedstocks for additive manufacturing of ti6al4v parts by material extrusion, Materials 16 (2023) 3162, https://doi.org/10.3390/ma16083162.
[21] D. Nötzel, T. Hanemann, New feedstock system for fused filament fabrication of sintered alumina parts, Materials 13 (2020) 4461, https://doi.org/10.3390/ma13194461.
[22] T. Heim, F. Kern, Influence of the feedstock preparation on the properties of highly filled alumina green-body and sintered parts produced by fused deposition of ceramic, Ceramics 6 (2023) 241–254, https://doi.org/10.3390/ceramics6010014.
[23] C. Carrot, A. Bendaoud, C. Pillon, Polyvinyl Butyral, Routledge Handbooks Online, 2015, https://doi.org/10.1201/b19190-4.
[24] K.E. Howard, C.D.E. Lakeman, D.A. Payne, Surface chemistry of various poly(vinyl butyral) polymers adsorbed onto alumina, J. Am. Ceram. Soc. 73 (1990) 2543–2546, https://doi.org/10.1111/j.1151-2916.1990.tb07632.x.
[25] Kuraray, Mowital ® – PVB RESIN, (2018).
[26] J. Gonzalez-Gutierrez, S. Cano, S. Schuschnigg, C. Kukla, J. Sapkota, C. Holzer, Additive manufacturing of metallic and ceramic components by the material extrusion of highly-filled polymers: a review and future perspectives, Materials 11 (2018) 840, https://doi.org/10.3390/ma11050840.
[27] G. Chen, P. Cao, G. Wen, N. Edmonds, Debinding behaviour of a water soluble PEG/PMMA binder for Ti metal injection moulding, Mater. Chem. Phys. 139 (2013) 557–565, https://doi.org/10.1016/j.matchemphys.2013.01.057.
[28] Informationszentrum Technische Keramik, ed., Brevier Technische Keramik, 4. Aufl, Fahner, Lauf, 2003.
[29] N.A. Conzelmann, L. Gorjan, F. Sarraf, L.D. Poulikakos, M.N. Partl, C.R. Müller, F. J. Clemens, Manufacturing complex Al2O3 ceramic structures using consumer-grade fused deposition modelling printers, Rapid Prototyp. J. 26 (2020) 1035–1048, https://doi.org/10.1108/RPJ-05-2019-0133.
[30] Almatis GmbH, ed., Global Product Data - CT 3000 LS SG, (n.d.).
[31] W.-W. Yang, M.-H. Hon, In situ evaluation of dimensional variations during water extraction from alumina injection-moulded parts, J. Eur. Ceram. Soc. 20 (2000) 851–858, https://doi.org/10.1016/S0955-2219(99)00221-6.
[32] S.Md Ani, A. Muchtar, N. Muhamad, J.A. Ghani, Binder removal via a two-stage debinding process for ceramic injection molding parts, Ceram. Int. 40 (2014) 2819–2824, https://doi.org/10.1016/j.ceramint.2013.10.032.
[33] M. Desloir, C. Benoit, A. Bendaoud, P. Alcouffe, C. Carrot, Plasticization of poly (vinyl butyral) by water: glass transition temperature and mechanical properties, J. Appl. Polym. Sci. 136 (2019) 47230, https://doi.org/10.1002/app.47230.